Eur. Phys. J. Plus (2022) 137:798
https://doi.org/10.1140/epjp/s13360-022-02995-y

THE EUROPEAN PHYSICAL JOURNAL PLUS

Regular Article

Investigation of the effects of mechanical and underfloor heating systems on the COVID-19 viruses distribution

Ali Niknahad[1], **Esmail Lakzian**[1,2,a], **Arastoo Saeedi**[3]

[1] Center of Computational Energy, Department of Mechanical Engineering, Hakim Sabzevari University, Sabzevar, Iran
[2] Peoples' Friendship, University of Russia (RUDN University), 6 Miklukho-Maklaya Street, 117198 Moscow, Russian Federation, Russia
[3] Head of Imam Ali Clinic, Oil Industry Health Organization, Shiraz, Iran

Received: 23 May 2022 / Accepted: 22 June 2022

Abstract Investigation of the spread of pollutants and especially pathogenic particles in the interior of today's buildings has become an integral part of the design of such buildings. When the Coronavirus is prevalent in the world, it is necessary to pay attention to the spread of the virus in the interior of residential apartments. In the present study, the Coronavirus particles emitted from the sneezing of a sick person in the bedroom of a residential apartment were tracked. Meanwhile, the degree of exposure of a mannequin that has been placed in the living room playing the role of a healthy person is examined. In this research, a segregated solution of steady-state flow and an unsteady particle solution have been separately used: a suitable, accurate, and optimal solution in particle studies. A comparison of the results shows that underfloor heating creates a healthier space around the healthy person's respiratory system, but instead, we will see more polluted areas around the sick person. According to the PRE results, the PRE value for a mechanical heating system is higher than a floor heating system. Therefore, it is recommended to use mechanical heating system in the apartments where the person with COVID-19 is hospitalized.

List of symbols

C	Particle concentration
C_c	Cunningham factor
C_p	Constant pressure special heat
$C_\eta = 85$ ،$C_1 = 0.25$ ،$C_T = 6$، $C_2 = 0.45$ ، $C_l = 1.4$، $\sigma_{v2} = 1$ ،$C_\mu = 0.22$	Model's constants
F_b	Buoyancy force
F_{bi}	Brownian force
F_D	Particle drag force
F_l	Lift force
F_n	Forces on particle
F_{th}	Thermophoresis force
F	Elliptic relaxation function
G	Gravity constant
K	Conductivity constant
K_B	Boltzmann constant
Kn	Knudsen number
L	Turbulent length scale
M_p	Particle mass
P	Pressure
T	Temperature
T_t	Turbulent time scale
T	Time
U_p	Particle velocity
U_i	Velocity component
$u_i^{'}$	Fluctuating velocity component

[a] e-mail: e.lakzian@hsu.ac.ir (corresponding author)

Published online: 10 July 2022

$\overline{u}_{\mathrm{I}}$	Average velocity component
V	Volume
X, y, z	Position components

Greek symbols

A	Prandtl number
B	Volume expansion factor
Δ_{ij}	Kronecker delta
Λ	Mean free path
M	Dynamic viscosity
N	Kinematic viscosity
N_t	Turbulent kinematic viscosity
P	Density
P_p	Particle density

1 Introduction

The emission of pollutant particles in the work and living environment can reduce the quality of respiratory air and cause serious diseases. In the meantime, virus particles are of particular importance. To study the particle diffusion of viruses, knowledge of their physics is necessary to begin the study. It is also essential to know the aerodynamics of the spread of viruses. In the following, the particle physics of the COVID-19 virus and the aerodynamics of its propagation are studied.

In the first step, the method of vaccination in the communities will be examined in order to see the importance of the issue of the Corona epidemic and the sensitivity of different governments to the issue of the COVID-19 epidemic. As Reno et al. [1] stated, the vaccination attention augmented beginning in Mars 2021. The vaccine attention development rate had a parallel configuration through districts. A method containing actions such as demanding masks and a "Green Pass" to go into interior spaces correspondingly aids prevent the epidemic. Now that the importance of vaccination has been clarified, the actions of governments in this regard must also be determined. Gillespie et al. [2] declared that vaccine providing was deferred by the Federal direction's favor, in order to support the native manufacturers. The early difficulties of the vaccine rollout started from an unsuccessful trial with outsourcing which began at the peak of the disaster.

In the second step, we will study and research previous works related to understanding the nature of COVID-19 viruses. These studies will provide accurate information about the nature of the virus to accurately simulate it numerically.

Egbuna et al. [3] stated that numerous different plans let and ease SARS-cov-2 to escape antiviral innate resistant tools. Ecological effluence not only eases SARS-cov-2 pollution but also rises infection-associated casualty danger. Some of the contaminants perform as endocrine disruptors, β-adrenergic receptors agonist blockers, and oxidative stress inducers, and they can create genomic changes in DNA and epigenetic reprogramming through total DNA methylation, gene-specific methylation, and microrna appearance. Development of contaminants created anxiety in Nigeria, and both the environment and human community were endangered [4]. Knowing the virus alone is not enough and the impact of the virus and the type of treatment on all ages should be considered. Older people are the most important category. Abbaspur et al. [5] stated that the information examination exhibited that all the m-health involvements had optimistic belongings on the wellbeing of the aged people. The m-health facilities for the senior people throughout the present epidemic were used for remedy, info providing, support, nursing, and psychological healthiness meeting targets. The consequences correspondingly showed that numerous issues affected the aged people's consumption of m-health. Finding the source of the virus is very effective in the treatment and prevention of the epidemic. Viruses can be of human or animal origins. Coronavirus is in the category of viruses with animal origin. As declared by Scharfman et al. [6], genomic examination exposed that this virus was phylogenetically connected to severe acute respiratory syndrome-like bat viruses, so bats might be the likely primary source. Using this information, researchers can make a serum and eventually an effective drug. Loa et al. [7] declared that the disparity of anti-tcov antiserum was improved. The consequences showed that Sephacryl S-1000 chromatography was valuable for the sanitization of tcov. By Cascella et al. [8], a study detailed the etiology of Coronavirus, transmission, epidemiology, pathophysiology, histology, history and physical nature, assessment, treatment and management of the disease, differential diagnoses, related studies, ongoing testing, prognosis, complications, inhibition, and patient education. It had improved the performance of the health team. The genome showed a series of similarities of more than 99.9% with COVID-19. The series similarity of COVID-19 with SARS-cov, and MERS-cov was 77.5% and 50%, respectively [9].

In the third step, understanding how pollutants are dispersed and how they settle will be examined. Understanding these principles will help to understand the theory used to simulate COVID-19 pathogenic particles. Nanoparticle chasing study by Kim et al. [10] is a technique for fast approximation of virus concentration in various testers. It could deliver a superior vision into the tester grade, concerning the level of virus accumulation. Many of the methods used in the field of particle tracking are experimental. For

example, a static light scattering centered technique for the quantification of virus spots had been adopted. The technique involved: first determining the concentration of the light distributed by viruses deferred in an aqueous solution and second determining the concentration of the light distributed by polymeric nanoparticles of identified concentration and similar size with the examined virus spot [11]. Furthermore, a standardized rate theory model was established by Makra et al. [12]. To define the time rate of change of the diameter of a round spot, diffusion-organized scratching of the kinetic form $\bar{r}^3 \sim$ Kt connecting the average spot diameter to the time was conserved. In addition to diffusion, other factors can affect the motion of particles. Spot removal and relocation are chiefly inclined by the spot possessions, the air circulation circumstances, and the airflow configurations in the two ventilated zones. Lighter spots have a superior impact on the interior air feature than do the heavier ones [13]. For weak dispersals of round Nano spots, Pecora [14] stated, the deterioration amount of the time autocorrelation of these intensity vacillations was applied to measure the spot dispersion factor. PCS was a commonly used approach for measuring the radius of small dimension spots in fluid dispersals. In FPI, the frequency expansion of beam dispersed by the spots was examined. Virus particles, like other particles, can form nuclei in the presence of water vapor. If a spot growing by vapor liquefaction happened in the moist area by the air/water edge, then the sedimentation speed for spots with a radius of about 1 pm was expected to be free of spot size and identical to the controlling value set by atmospheric turbulence [15]. Chen et al. [16] stated that the well-mixed postulation cannot hold for large spots. A model by Lai and Chen delivers a well-organized and trustworthy means for examination of spatial and time-based spot concentration in fields and the consequence will be precious for refining present realization of humanoid contact valuation.

In the fourth step, the distribution of infectious salivary particles will be studied in the literature. These provide the basis for simulating and studying Coronavirus particles in salivary secretions in the present study. Experimental imaging is also popular for saliva particles. Actual shadowgraph imaging was applied by Tang et al. [17] to envisage high-speed descriptions of healthy persons sneezing and breathing. The maximum observable space over which the sneeze clouds moved was 0.6 m, and, also, its top speed was 4.5 m/s. The extreme zone of spreading was 0.2 m. The excessive zone growth rate was 2 m /s. The outer spreading space and speed were 0.6 m and 1.4 m/s, respectively, for breathing from the nose. Saliva particles can cause many problems. Coughs and sneezes might have pathogen-bearing drops of mucosalivary liquid. So, they might spread many contagious illnesses. Fragmentation of the liquid into drops continued to happen outer of the breathing zone through forceful breaths. Such fragmentation includes multifaceted steps of events from sheets, to bag bursts, to ligaments, and lastly broken into drops [18]. Li et al. [19] stated the vapor forms a “vapor cloud" in front of the breathing path opening. This considerably blocked the vaporization of the drops. Drop dimension decrease caused by vaporization increases the concentration of midair drops. Parametric investigations were done to assess the causes affecting drop vaporization. Today, with the advent of high-speed supercomputers, the use of CFD methods to track particles is much more costly and time-effective than experimental methods. Cravero et al. [20] declared that the spit drop spray ejected through inhalation, or coughing is the chief reason for the spread of the SARS-Cov-2. Also, Lagrangian and Eulerian numerical methods can be applied to model the coughing and the inhalation occasions. CFD was used for modeling of COVID-19 spreading in an aircraft cabin, an elevator, a schoolroom, a shop, an operational room of a clinic, a cafeteria, a clinic waiting room, and a children’s recovery chamber in a clinic [21]. CFD was applied for modeling a classroom containing a sick person with COVID-19 by Mirzaie et al. [22]. Using the bench dividers for persons can avoid the contagion of Coronavirus to some range in a classroom. An upsurge in the air circulation velocity amplified the drops’ paces in the airflow path, instantaneously decreasing the residence time of the drops by blockades. Drops with radius less than 125 μm are most accountable for the diffusion of the Coronavirus [23]. Though floating transmission has been measured as a probable way for the blowout of Coronavirus, the part that sprays play in Coronavirus spread is still debatable. The analysis exposed that 2.3% of the air tasters and 9.3% of the surface tasters were positive, showing that the separation regions were contaminated with the Coronavirus. Due to the fact that Coronavirus particles are highly contagious in the environment, it is necessary to use an efficient particle removal system. The application of ceiling-mounted air cleaners is operative in decreasing the floating diffusion of Coronavirus in these zones [24]. Wet steam studies can also be used to conduct research related to Coronavirus and salivary particle dispersion. In the meantime, it is very important to study the particle-moisture parameters and its relationship with other parameters. Salmani et al. [25] stated that the drop-moisture factor can be found as a dimensionless quantity which is a function of operative factors. A dimensionless drop diameter can be found as a function of a resistance factor, which is also a dimensionless factor [26].

Lack of accurate knowledge of how the Coronavirus particles spread in residential environments can cause problems for the occupants of the building where a person with Coronavirus is present. Numerical examination of the Coronavirus particle trajectory in a building, in addition to reducing the cost of experimental studies, can provide an accurate understanding of how particles propagate. In this study, the spread of Coronavirus in a residential apartment with underfloor and mechanical heating systems after sneezing of a hospitalized person in a bedroom is investigated. A mannequin is placed in the living room playing the role of a healthy person. The concentration of pathogenic particles around this person’s respiratory system when using each of these heating systems has been studied and compared. The ability of heating systems to remove particles has also been studied. By understanding which system is less capable of removing particles, it will provide a solution to improve the particle removal performance so that residents can continue to enjoy the benefits of that system. Interesting innovations have been used in this research. As is clear from aerosol science, particles are affected by different forces. In this study, all forces on fluid particles, including Brownian, weight, buoyancy, Stokes drag, Saffman lift, diffusion, thermophoresis, and turbophoresis, were evaluated. Other innovations in this study compared to the work of the past are the simulation of thermal plume around the body of mannequins and its effect on the distribution of particles, as well as the simulation of flow caused by sneezing. In addition, in this study, a geometry has been studied that plays an

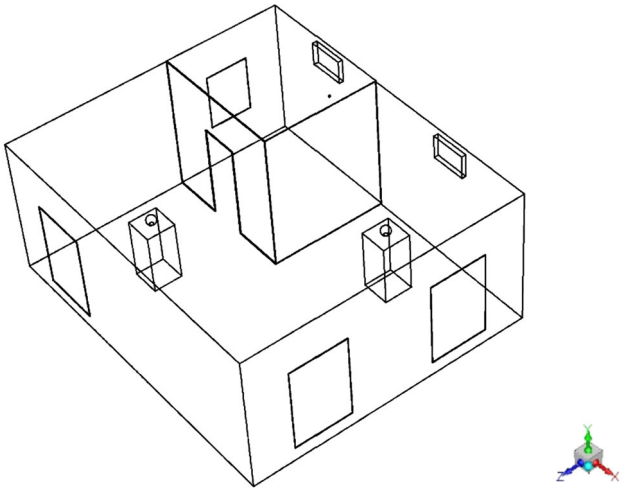

Fig. 1 Perspective view of the apartment under investigation

important role in people's daily lives. Therefore, the present work can be considered as a complete and comprehensive work in the field of spreading the Coronavirus inside the building.

2 Problem definition and the governing equation

In the present study, the continuity, momentum, and energy equation after determining the solution plane, approximation method, discretization, boundary condition, and initial guess are solved to obtain the desired flow field. The forces on particle equations are solved by the Lagrangian method. The solution of the discrete phase is conducted by determining the physical properties such as density, diameter, injected particle in unit time, injection locations, the initial velocity of particles, and forces acting on particles. Discrete phase solution is performed in the unsteady formulation. 40,000 particles per second with 0.001 s time step for a 0.15-s duration are injected into the domain. The particle diameters in this study are 0.15, 0.5, 1, 1.5, 2, 2.5, 3, 3.5, 4, 4.5, 5 microns that each category contains 10% of total particles. Also, in this study, the size of COVID-19 viruses is considered 150 nm, and the density of each virus is about 1000 kg/m3 [7]. Weight, drag, buoyancy, lift, thermophoresis, turbophoresis, diffusion, and Brownian forces are considered. The objective of the present study is to find the distribution of Coronavirus injected by sneezing in a 44-square-meter apartment. In the bedroom, a sick person stands toward the door. At this time, this person sneezes toward the door and injects particles with a temperature of 39 °C and a velocity of 4.5 m/s with 0.150 s duration that injects 40,000 particles [27]. The wall discrete phase boundary condition is selected as a trap that causes prevent the reflection of colliding particles. In the living room, a healthy person with a body temperature of 37 °C is standing. One objective of this study is to investigate infectious particle distribution around a healthy manikin respiratory system. In this problem, the condition of one wintery night is considered at which a hot air duct heating system producing flow with 1 m/s and 26 °C is working [28]. A floor heating system is also considered a choice. The floor heating system maintains the floor of the apartment at a constant temperature of 26 °C. The objective is to find the effect of the heating system on particle distribution. The outside temperature is 5 °C. For modeling the turbulence, the v2f model is used [29]. Figure 1 shows a schematic view of the system.

The summation of all forces determines the trajectory of the particle. These forces are gravity, buoyancy, buoyancy, drag, lift, diffusion, thermophoresis, turbophoresis, and Brownian [29].

$$\frac{d\overline{u}_P}{dt} = F_D + F_L + F_b + f_{bi} + F_t + F_w + \cdots \tag{1}$$

In this study, the finite volume method is used for discretization.

3 Flow governing equations

Continuity is solved simultaneously with the momentum equation to find the flow field pressure and velocity. The reduced form for incompressible turbulent flow is [29]:

$$\frac{\partial \overline{u}}{\partial x} + \frac{\partial \overline{v}}{\partial y} + \frac{\partial \overline{w}}{\partial z} = 0 \tag{2}$$

Table 1 Boundary conditions

Particle condition	Temperature condition(C)	Flow	Boundary type	Zone
(Escape)	26	0 and 1 m/s	Velocity inlet	Inlet
(Escape)	5	1 atm	Pressure outlet	Outlet
(Trap)	Adiabatic	No-slip	Wall	Building wall
(Trap)	26	No-slip	Wall	Floor
(Escape)	39	4.5 m/s	Injection	Sick person
(Trap)	37	No-slip	Wall	Healthy person

Based on the second law of Newton and considering surface and volume forces and simplifying, the momentum conservation equation is obtained. This equation states the summation of forces on a fluid particle equals momentum changes. By Considering constant viscosity and incompressible turbulent flow, one can simplify this equation and finally obtain [29]:

$$\overline{u}\frac{\partial \overline{u}}{\partial x}+\overline{v}\frac{\partial \overline{u}}{\partial y}+\overline{w}\frac{\partial \overline{u}}{\partial z}+\frac{1}{\rho}\frac{\partial \overline{p}}{\partial x}=\nu(\nabla^2\overline{u})-\frac{\partial\overline{(u')^2}}{\partial x}-\frac{\partial\overline{(u'v')}}{\partial y}-\frac{\partial\overline{(u'w')}}{\partial z} \tag{3}$$

According to the geometry understudy, the flow-through apartment is turbulent and needs a turbulence model to be solved. In this study, the v2f model is used. Two equations of this model demonstrate turbulent kinetic energy and dissipation, and the other two equations demonstrate turbulent viscosity and elliptic relaxation function. By coupling these equations with governing equations, one can predict the turbulent behavior of the flow variable.

In v2f, turbulent viscosity is defined as [29]:

$$v^2=C_\mu v^2 T \tag{4}$$

The Reynolds transition equation for v2f [29]:

$$\frac{\partial\overline{v^2}}{\partial t}+U_i\frac{\partial v^2}{\partial x_j}=kf-\left(\frac{v^2}{k}\right)\varepsilon+\frac{\partial}{\partial x_j}\left[\left(\nu+\frac{\nu_t}{\sigma_{\overline{u2}}}\right)\frac{\partial v^2}{\partial x_j}\right] \tag{5}$$

The elliptic relaxation function [29]:

$$L^2\nabla^2 f-f=\left(\left(\frac{(C_1-1)}{T}\right)\left(\frac{v^2}{k-\frac{2}{3}}\right)-\frac{C_2P_k}{\varepsilon}\right) \tag{6}$$

Turbulent length scale [29]:

$$L=C_l\max\left[\left(\frac{k^{3/2}}{\varepsilon}\right),\ C_n\left(\frac{\nu^3}{\varepsilon}\right)^{\frac{1}{4}}\right] \tag{7}$$

Turbulent time scale [29]:

$$\mathrm{T_t}=\max\left[\left(\frac{k}{\varepsilon}\right)\left(C_T\left(\frac{\nu}{\varepsilon}\right)^{\frac{1}{2}}\right)\right] \tag{8}$$

The constants in proceeding equations are:

$$C_\eta=85,\ C_l=0.25,\ C_T=6,\ C_2=0.45,\ C_1=1.4,\ \sigma_{v2}=1,\ C_\mu=0.22 \tag{9}$$

In the present study, to solve the momentum and energy equations in a coupled way for simulating the free convection, the incompressible perfect gas equation is used [29].

$$\rho=\frac{P_{op}}{\frac{R}{M_w}T} \tag{10}$$

The turbulent form of the energy equation is [22]:

$$\frac{\partial\overline{T}}{\partial t}+\frac{\partial(\overline{uT})}{\partial x}+\frac{\partial(\overline{vT})}{\partial y}=\frac{\partial}{\partial x}\left(\frac{K}{\rho C_p}\frac{\partial\overline{T}}{\partial x}\right)+\frac{\partial}{\partial y}\left(\frac{K}{\rho C_p}\frac{\partial\overline{T}}{\partial y}\right)-\left[\frac{\partial(\overline{u'T'})}{\partial x}\frac{\partial(\overline{v'T'})}{\partial y}\right] \tag{11}$$

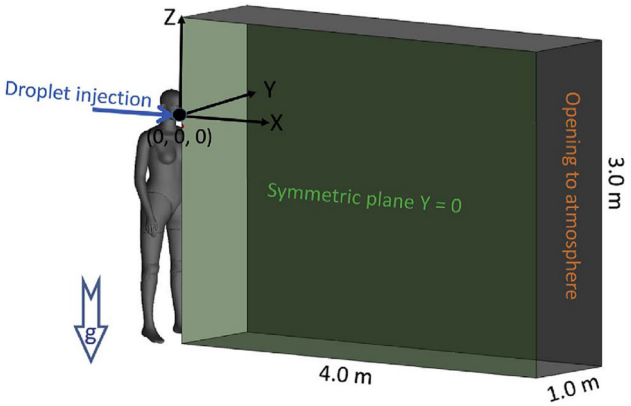

Fig. 2 The geometry of Li and Shang's study [19]

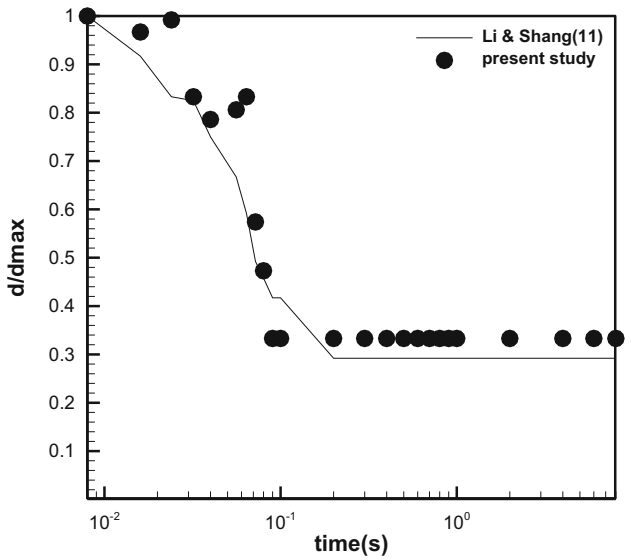

Fig. 3 Comparison of mean diameter in the present work with Li and Shang study [19]

Table 2 Mesh independency according to maximum temperature and maximum velocity

Maximum temperature(K)	Maximum velocity(m/s)	Cell number
297.09	0.13	1,000,000
300.09	0.13	2,000,000
300.10	0.13	3,000,000

4 Discrete phase governing equation

If the body is completely immersed in a fluid, the normal force acting on it equals the weight of the fluid displaced by the body [29].

$$F_b = \rho g v \tag{12}$$

Small particles in the shear layers are subjected to a force perpendicular to the current called the Saffman lift force. The relation for calculating this force is given in Eq. 13 [29].

$$F_{L(saff)} = 1.615 \rho v^{0.5} d^2 (u^f - u^p) \left| \frac{du^f}{dy} \right|^{0.5} \operatorname{sgn}\left(\frac{du^f}{dy} \right) \tag{13}$$

The drag force applied to small particles is obtained through the Stokes drag force relation given in Eq. 14 [24].

$$F_D = 3\pi\mu \left(u^f - u^p \right) d_p \begin{cases} u^f - \text{fluid} - \text{velocity} \\ u^p - \text{particle} - \text{velocity} \end{cases} \tag{14}$$

Equation 15 shows the equal mass of each particle. The concentration also is the total mass of particles divided by the total volume, as shown in Eq. 15 [29].

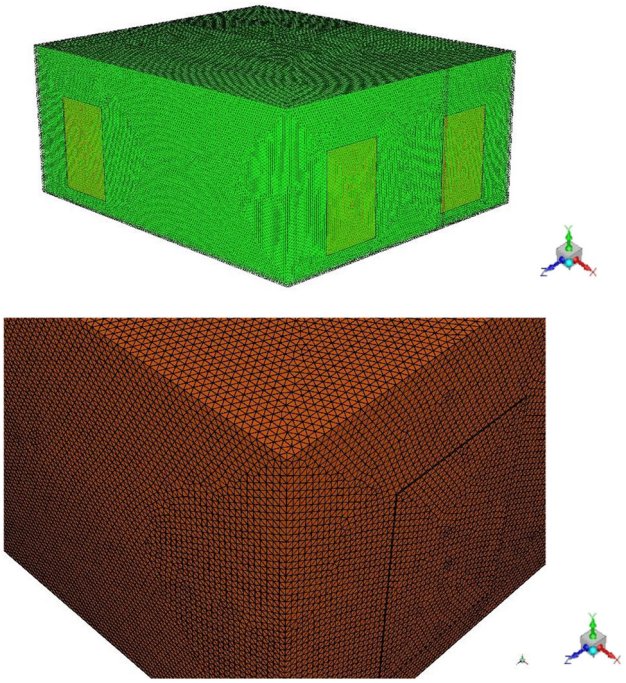

Fig. 4 Grid used in the present study

$$m_p = V_p \rho_p$$

$$C = \frac{m_p \sum_{j=1}^{n} N_{(i,j)}}{V_i} \tag{15}$$

Brownian movement is the accidental movement of spots in a fluid [29].

$$F_{bi} = \frac{\xi_i \sqrt{\pi}\, S_0}{\Delta t}$$

$$S_0 = \frac{216 \nu K_B T}{\pi 2 \rho d_d^2 \left(\rho_p / \rho\right)^2 C_C} \tag{16}$$

Thermophoresis is detected in blends of moveable spots where the distinct spot categories display different reactions to the temperature gradient force. The term thermophoresis is frequently used for aerosol blends, but can generally denote the occurrence in all phases [29].

$$F_{\text{th}} = -\frac{1}{2} \frac{\pi \mu v d^2 \nabla T}{\lambda T} \tag{17}$$

To evaluate the efficiency of a ventilation system and apartment surfaces capability for maintaining the indoor air quality in a safe range, the particle removal efficiency is used, and Eq. 18 states the proper relation [29].

$$\text{PRE} = \frac{C_0 - C}{C_0} \times 100 \tag{18}$$

Table 1 shows all the boundary conditions used in the present study.

5 Solution method

The solver in the present study is FLUENT 6.3.26, which can discretize the equation of flow and also solve the DPM equations. First, using a segregated solver, equations of flow are solved, and then DPM equations are solved in the domain. This method has less computational cost than simultaneously solving flow and DPM equations. In the present study, for velocity–pressure coupling, the SIMPLE method is selected.

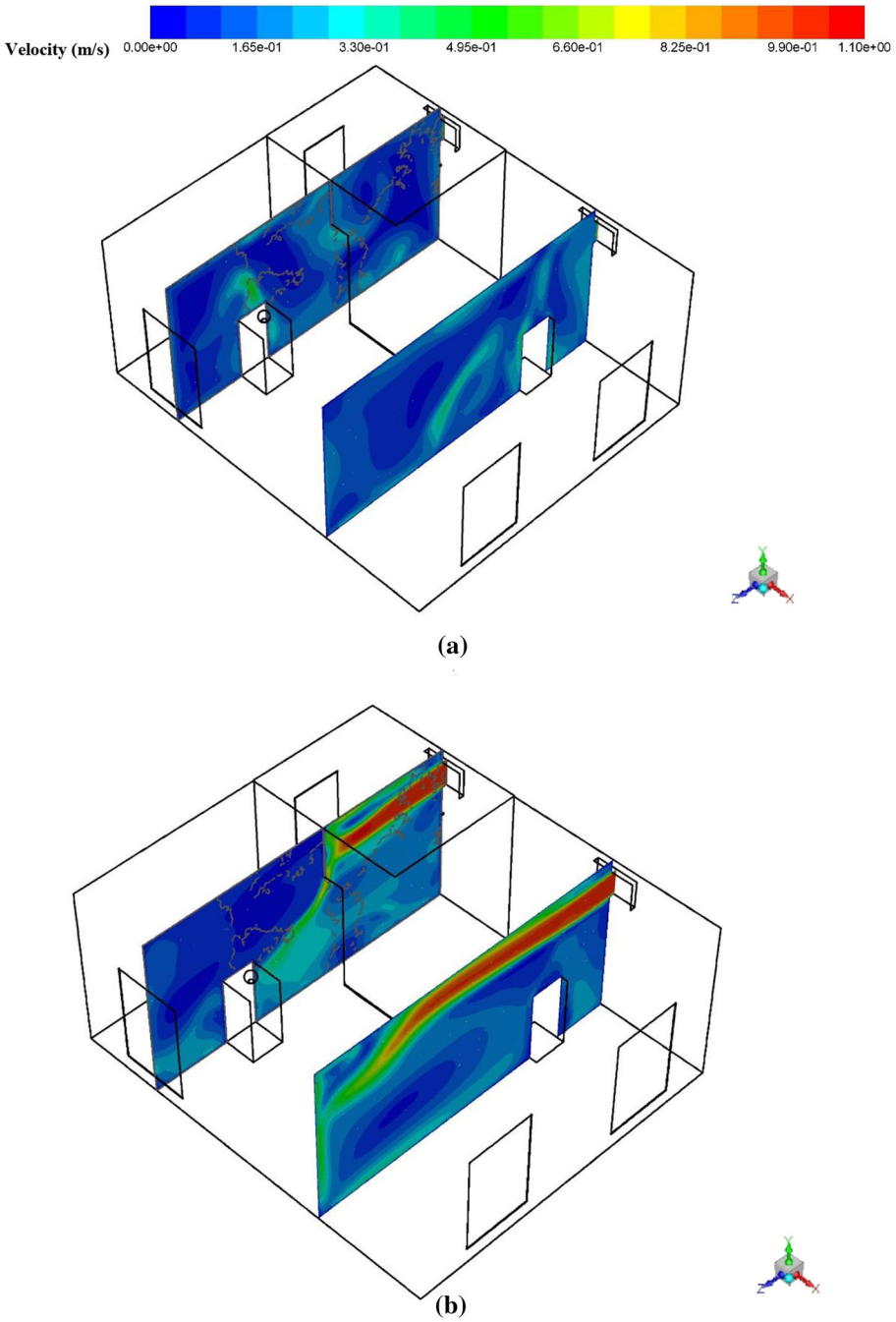

Fig. 5 Velocity distribution in a one-bedroom apartment **a** when using underfloor heating, **b** when using mechanical heating

6 Results and discussion

6.1 Validation

In the present section, the results of validation with Li et al. [19] are described. The geometry of the system is depicted in Fig. 2. Their study engaged a Eulerian–Lagrangian method to simulate the vaporization and spreading of drops. Figure 3 shows the mean diameter comparison with the present work and Li et al. [19]. The comparison shows good agreement, and the trend is captured very well.

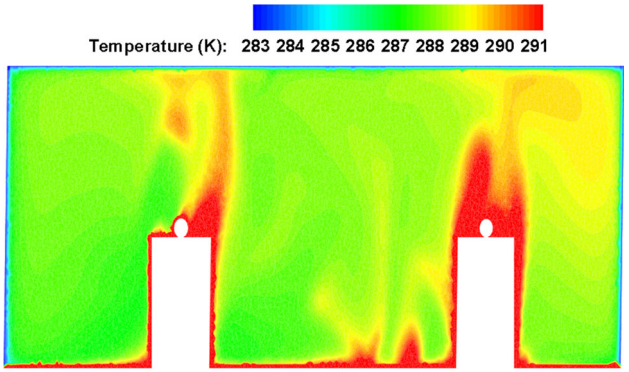

Fig. 6 Display of thermal plume around the body of the mannequins

6.2 Independency of grid

In this section, the appropriate grid number for calculation is obtained. For finding the threshold of grid independency, mean temperature and mean velocity are considered. Comparing the obtained results, 2,000,000 cells grid structure is selected for computation. The results are shown in Table 2. It is noteworthy that the amount of y^+ in this study is much less than one.

To better understand the meshing used in the present study, the graphic view of the grid used is shown in Fig. 4.

6.3 Velocity and particle distribution and sedimentation

Figure 5 shows the velocity contour in a one-bedroom apartment when an underfloor heating system and a mechanical heating system are used. When the underfloor heating system is used, a uniform and smooth flow is formed in the whole environment of the apartment. In this case, the maximum speed in the computational domain is estimated at about 0.5 m per second. Around the mannequins, due to the extreme temperature gradients, the air velocity due to free movement is higher than in other areas. When using the mechanical heating system, the air comes out of the air conditioner duct at a speed of 1 m per second. In this case, hot air is rapidly distributed in the building and carries with it the temperature and subsequently the particles in the space.

In this work, unlike previous works, the effect of thermophoresis is considered in all parts of the room. One of the most important parts that is the basis of the present study is around the mannequins, especially their respiratory system. In this study, the thermal plume around the mannequins is modeled and the effect of the temperature gradient around the mannequins on the particle trajectory is considered. Therefore, all the results include the effect of this phenomenon. Figure 6 shows the temperature contour around the mannequins. What is comprehended from this figure is that heat is transferred from the floor of the room (underfloor heating system) and the body of the mannequins to the environment. There are extreme temperature variations around the mannequins that cause thermophoresis on the particles. There is also a severe thermal plume above the mannequins, which can affect the trajectory of the particles. It should be noted that this phenomenon has not been studied in similar works in the past.

Figure 7 shows the distribution of COVID-19 viruses' particles in a residential apartment in the presence of underfloor heating system at 5, 10, 25, 50, and 100 s after the patient sneezes. The result is that the particles stay around the sick person in the bedroom and do not spread to other parts of the apartment. The space inside the bedroom is heavily polluted, but instead, the accommodation of the mannequins is almost safe. Due to this figure, the number one mannequin is exposed to many virus particles and it is possible to get COVID-19, but the number two mannequin is almost in a safe place and does not pose a threat. Due to the weight of the Coronavirus particles, it is observed that the particles are pulled toward the floor of the building due to the force of weight. Thus, the force of gravity is greater than the force of Stokes drag. Since the temperature of the walls of the building is lower than the interior areas, a strong temperature gradient occurs in this area, which pulls the particles toward the walls and removes them. Therefore, thermophoresis is an effective force in removing particles in this state and its effect is greater than the Saffman lift force.

Figure 8 shows the distribution of COVID-19 viruses in an apartment equipped with a mechanical heating system at times 5, 10, 25, 50, and 100 s after the patient sneezes. The particles contaminated the entire building in about 50 s and left almost no safe space in the environment. The floor heating provides a safer place than a hot air duct, but the concentration at each equal time is much higher for floor heating than the hot air duct. This means floor heating system provides a safer place for living, but the pollution of particles near the source of pollution is higher than when mechanical ventilation is used. The most hazardous zones are the bedroom and in front of the bedroom door. The amount of pollution is higher in the lower areas of the apartment than in other areas due to the lower level of turbulence and the predominance of turbophosis when using the mechanical heating system. The floor heating provides a safer zone around the healthy manikin, and the risk of infecting the manikin with the COVID-19 virus is considerably lower. It is noteworthy that after 100 s from the start of particle release, almost half of the particles are removed from the environment by the mechanical heating system, which shows the high ability of this system to remove particles compared to the underfloor heating system. Also, due to the spread of particles in most areas of the apartment when using the mechanical heating

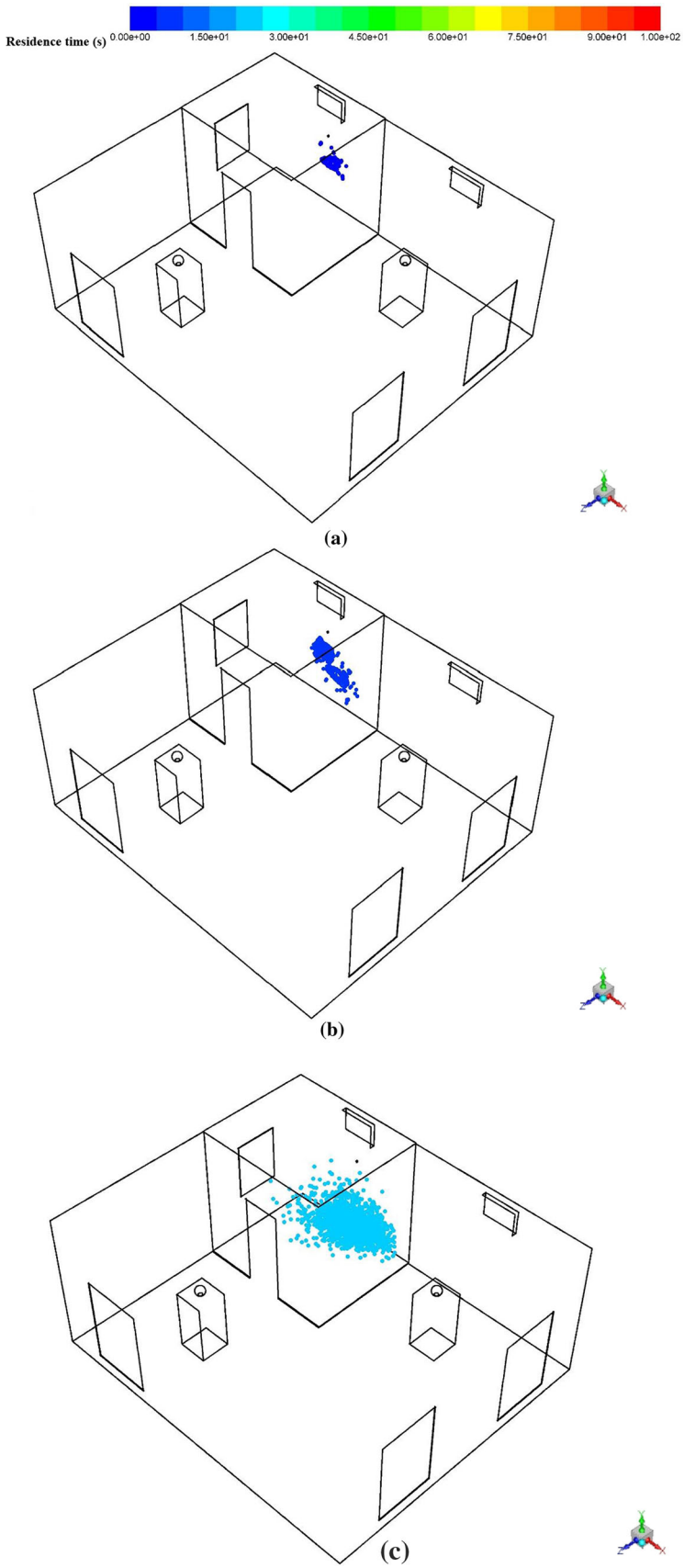

Fig. 7 The distribution of COVID-19 viruses' particles in a residential apartment in the presence of underfloor heating system at **a** 5, **b** 10, **c** 25, **d** 50, and **e** 100 s after the patient sneezes

Fig. 7 continued

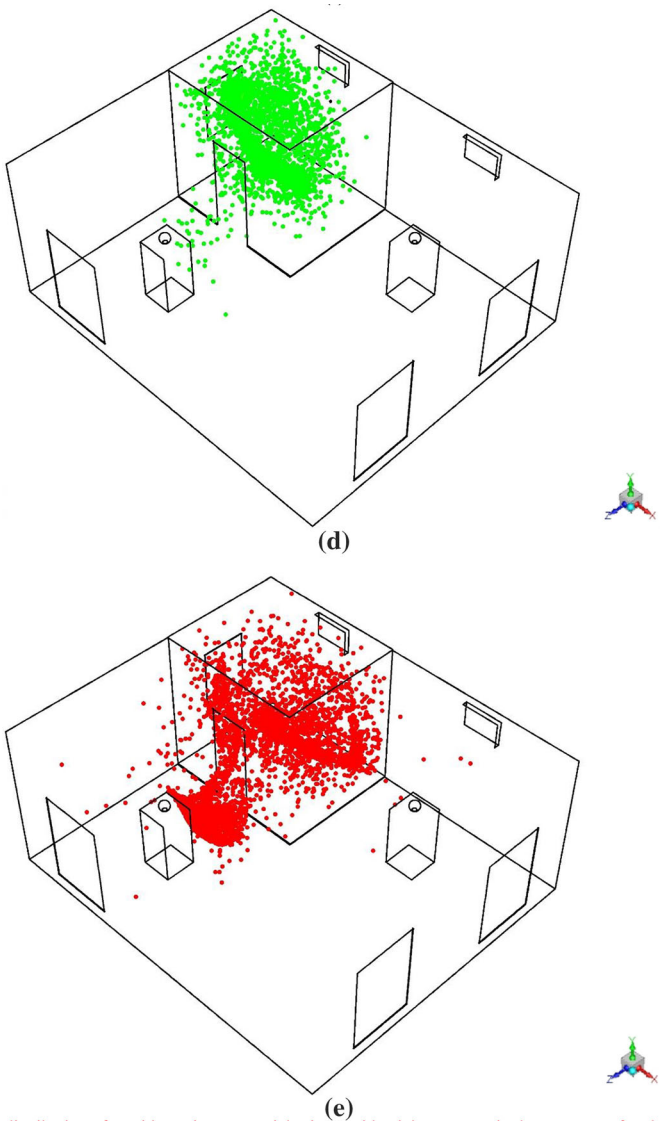

system, residents should leave the environment for at least 200 s after the environment is contaminated with polluting particles to avoid exposure to pathogens.

Figure 9 shows the C/C0 value around the respiratory system of manikin (mouth and nose) for the case of mechanical and floor heating systems. Based on this result, it can be concluded that after about 12.5 s after the release of particles in the case of mechanical heating system, the dimensionless concentration around the mannequin respiratory system is sharply increased and begins to fluctuate over time. The infectious particles in this area are absent all the time for the floor heating system.

6.4 Particle removal efficiency

Figure 10 shows the particle removal efficiency concerning both mechanical heating and floor heating systems. The particle removal efficiency offers the capability of the ventilation system to remove the particles from the environment. According to the PRE diagram, up to 20 s after release due to the dominance of weight force over other forces, the PRE floor heating system is higher than the PRE mechanical heating system. After this time, due to the dominance of other forces such as turbophorsis and drag, which are caused by the movement of high-velocity fluid in the environment, the PRE of the mechanical heating system increases. In 100 s after injection of PRE particles, the mechanical heating system is about 53.3% and the PRE floor heating system is only about 22.2%.

6.5 Improved ventilation when using underfloor heating

To reduce Coronaviruses in the building environment when the underfloor heating system is used, a low-power discharge fan (about 80 watts) is provided in the building. Using this small fan greatly reduces the time required to remove particles.

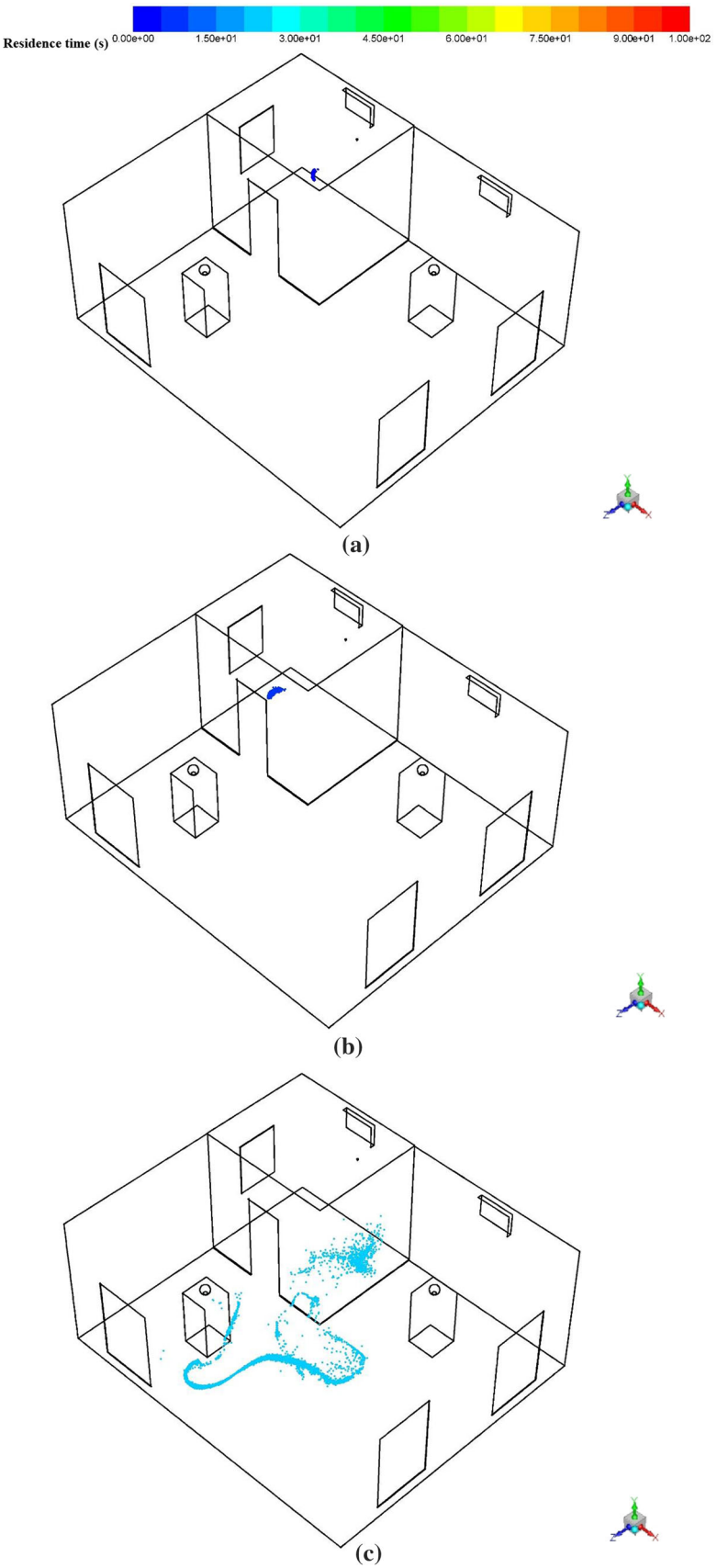

Fig. 8 The distribution of COVID-19 viruses' particles in a residential apartment in the presence of mechanical heating system at **a** 5, **b** 10, **c** 25, **d** 50, and **e** 100 s after the patient sneezes

Fig. 8 continued

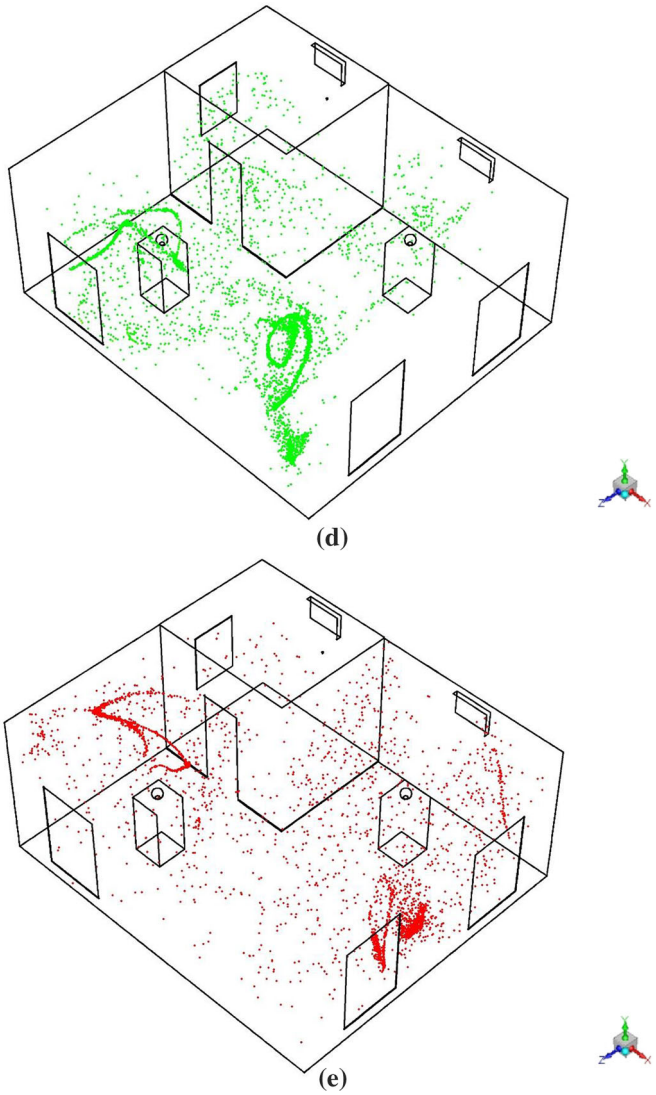

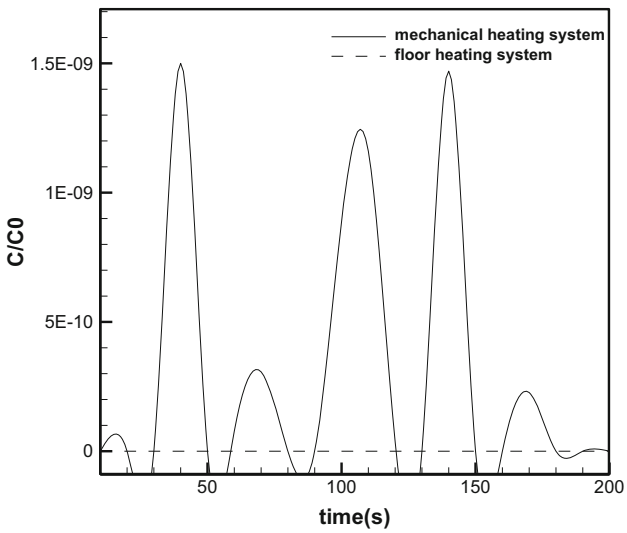

Fig. 9 C/C0 value around the respiratory system of manikin vs. time for mechanical and floor heating system

According to the results, the use of a fan with a power of about 80 watts greatly helps to reduce Coronavirus particles in the apartment environment when the underfloor heating system is used. Using this 80-W fan, the time required to remove particles in

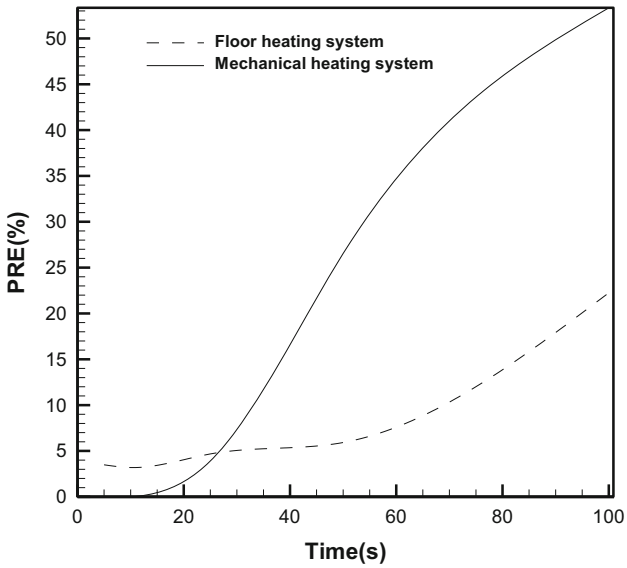

Fig. 10 The particle removal efficiency of mechanical and floor heating systems

the environment will be less than one second, which is very convenient. Therefore, ventilation system designers in such apartments are strongly advised to use a suitable exhaust fan inside the building to remove contaminants such as Coronavirus when underfloor heating system is being used. Figure 11 shows Coronavirus particles in the interior of the apartment at different times. According to the particle trajectory, in this case, the particles released from the person's mouth are drawn directly to the exhaust fan and removed from the environment. Unlike the previous cases, using a fan to ventilate the building completely removes Coronavirus particles in less than a second.

For comparison, the PRE diagram including the underfloor heating system with the exhaust fan is shown in Fig. 12. Based on these results, the PRE percentage has risen from 0 to 99.6% in about 0.75 s. If the underfloor heating system did not have an exhaust fan, this value would be less than 25% by 100 s after the particles were released. Accordingly, by using a small 80-W exhaust fan, the quality inside the building is greatly increased.

7 Conclusion

In this study, the distribution of sneeze particles from a COVID-19 suffering person on a wintery night is investigated in the presence of two alternative heating systems, namely a mechanical heating system and a floor heating system. Particles' diameters range from 150 nm to 5 microns and are injected during 150 microseconds. The buoyancy, weight, diffusion, drag, buoyancy, Saffman lift, turbophoresis, thermophoresis, and Brownian are considered. The important point that has been mentioned in the present work is that, unlike previous works, the thermal plume around the body of the mannequins and its effect on the trajectory of the virus particles has been considered. Finally, by understanding which system is less capable of removing particles, it will provide a solution to improve the particle removal performance so that residents can continue to enjoy the benefits of that system.

(1) In contrast to the mechanical heating system, the floor heating system provides a safer space, and particle distribution is much more limited than the mechanical system. Still, highly polluted areas in this kind of system are more noticeable than the mechanical heating system. Due to the spread of particles in most areas of the apartment when using the mechanical heating system, residents should leave the environment for at least 200 s after the environment is contaminated with polluting particles to avoid exposure to pathogens.
(2) When using underfloor heating system, due to the weight of the Coronavirus particles, it is observed that the particles are pulled toward the floor of the building due to the force of weight. Since the temperature of the walls of the building is lower than the interior areas, a strong temperature gradient occurs in this area, which pulls the particles toward the walls and removes them.
(3) The concentration at each equal time is much higher for floor heating than the hot air duct. The amount of pollution is higher in the lower areas of the apartment than in other areas due to the lower level of turbulence and the predominance of turbophosis when using the mechanical heating system. After 100 s from the start of particle release, almost half of the particles are removed from the environment by the mechanical heating system, which shows the high ability of this system to remove particles compared to the underfloor heating system.
(4) Results show the concentration of the infectious particles oscillates around the respiratory system of the manikin with time in the case of a mechanical heating system; in contrast, the infectious particles around the respiratory system of the manikin are absent all the time when the floor heating system is being used.

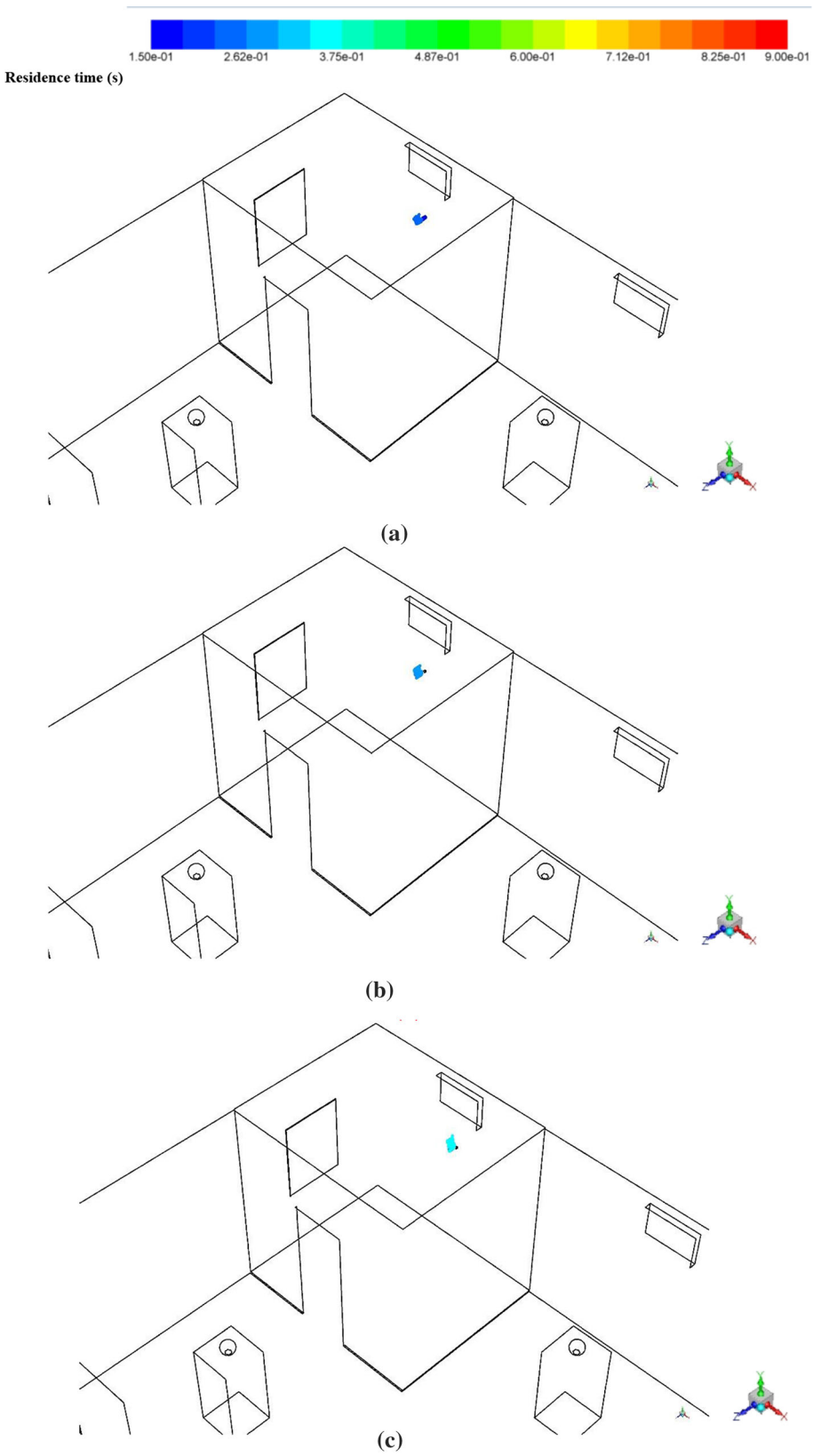

Fig. 11 The distribution of COVID-19 viruses' particles in a residential apartment in the presence of underfloor heating system equipped with exhaust fan at **a** 0.15, **b** 0.2, **c** 0.3, **d** 0.5, **e** 0.7, and **f** 100 s after the patient sneezes

Fig. 11 continued

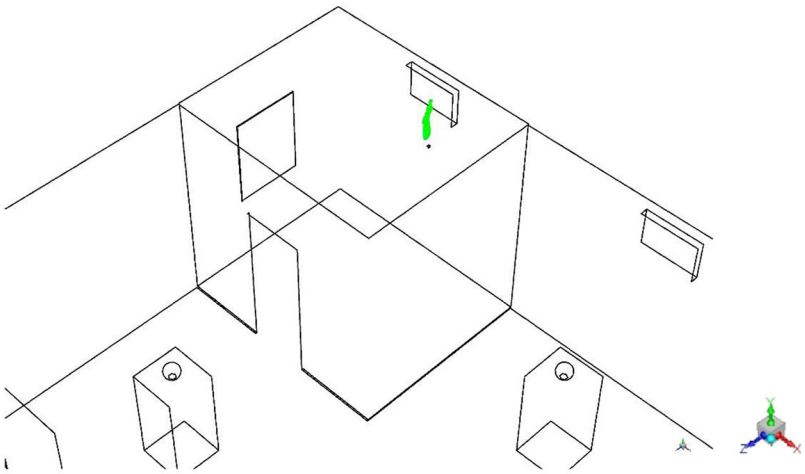

(d)

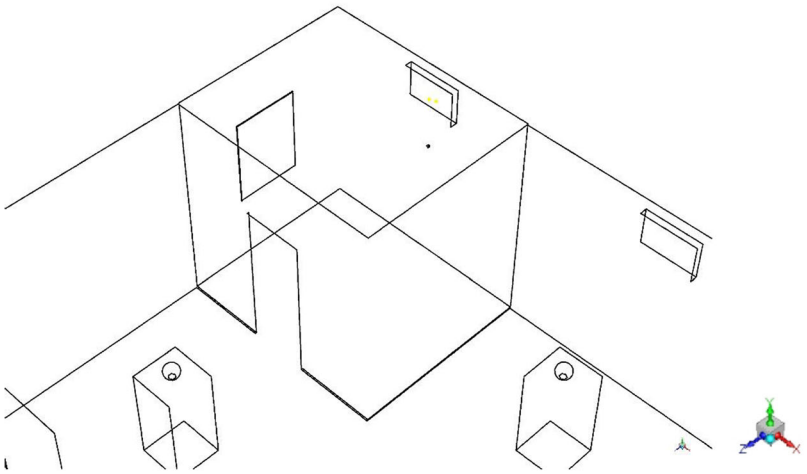

(e)

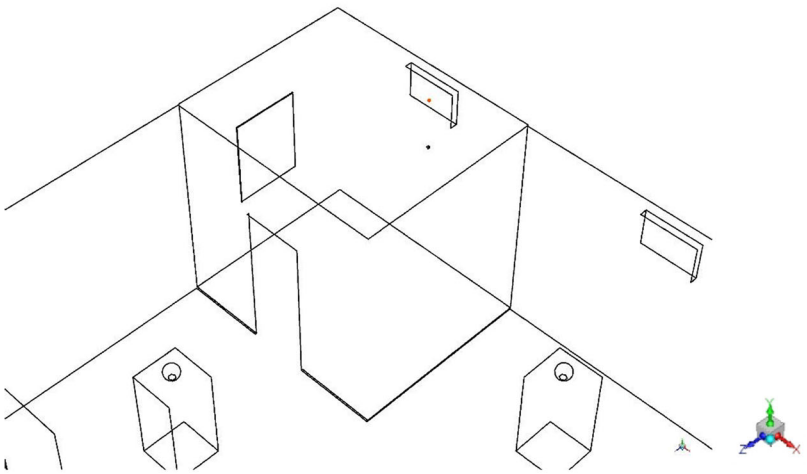

(f)

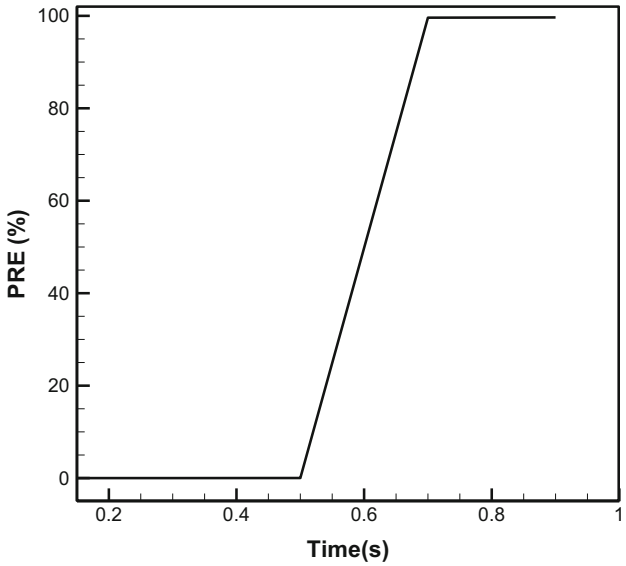

Fig. 12 The particle removal efficiency of floor heating systems with exhaust fan

(5) According to the PRE diagram, up to 20 s after release due to the dominance of weight force over other forces, the PRE floor heating system is higher than the PRE mechanical heating system. After this time, due to the dominance of other forces such as turbophorsis and drag, which are caused by the movement of high-velocity fluid in the environment, the PRE of the mechanical heating system increases. In 100 s after injection of PRE particles, the mechanical heating system is about 53.3% and the PRE floor heating system is only about 22.2%.

(6) Underfloor heating system provides a safer place for living, but the pollution of particles near the source of pollution is higher than when mechanical ventilation is used. To reduce Coronaviruses in the building environment when the underfloor heating system is used, a low-power discharge fan (about 80 W) is provided in the building. Using this 80 W fan, the time required to remove particles in the environment will be less than one second, which is very convenient. Therefore, ventilation system designers in such apartments are strongly advised to use a suitable exhaust fan inside the building to remove contaminants such as Coronavirus when underfloor heating system is being used.

Data Availability Statement The datasets generated during and/or analysed during the current study are available from the corresponding author on reasonable request. This manuscript has associated data in a data repository. [Authors' comment: All data included in this manuscript are available upon request by contacting with the corresponding author.]

References

1. C. Reno, F. Sanmarchi, M.A. Stoto, M.P. Fantini, J. Lenzi, D. Golinelli, Health Policy Technol. (2022). https://doi.org/10.1016/j.hlpt.2022.100604
2. J.A. Gillespie, J. Buchanan, C.H. Schneider, F. Paolucci, Health Policy Technol. (2022). https://doi.org/10.1016/j.hlpt.2022.100607
3. C. Egbuna, C.N. Amadi, K.C. Patrick-Iwuanyanwu, S.M. Ezzat, C.G. Awuchi, P.O. Ugonwa, O.E. Orisakwe, Environ. Toxicol. Pharmacol. (2021). https://doi.org/10.1016/j.etap.2021.103638
4. A.B. Engin, E.D. Engin, A. Engin, Curr. Opin. Toxicol. (2021). https://doi.org/10.1016/j.cotox.2021.03.004
5. S. Abbaspur-Behbahani, E. Monaghesh, A. Hajizadeh, S. Fehresti, Health Policy Technol. (2022). https://doi.org/10.1016/j.hlpt.2022.100595
6. B.E. Scharfman, A.H. Techet, J.W. Bush, L. Bourouiba, Aerobiology (2016). https://doi.org/10.1007/s00348-015-2078-4
7. C.C. Loa, T.L. Lin, C.C. Wu, T.A. Bryan, H.L. Thacker, T. Hooper, D. Schrader, J. Virol. Methods. (2002). https://doi.org/10.1016/S0166-0934(02)00069-1
8. M. Cascella, M. Rajnik, A. Aleem, S.C. Dulebohn, Di Napoli R. Features, evaluation, and treatment of coronavirus (COVID-19). Statpearls (2022) https://www.ncbi.nlm.nih.gov/books/NBK554776/
9. J.M. Kim, Y.S. Chung, H.J. Jo, N.J. Lee, M.S. Kim, S.H. Woo, S. Park, J.W. Kim, H.M. Kim, M.G. Han, Osong Public Health Res. Perspect. (2020). https://doi.org/10.24171/j.phrp.2020.11.1.02
10. P. Kramberger, M. Ciringer, A. Štrancar, M. Peterka, Virol. J. (2012). https://doi.org/10.1186/1743-422X-9-265
11. I. Makra, T. Péter, E.G. Róbert, MethodsX (2015). https://doi.org/10.1016/j.mex.2015.02.003
12. A.D. Brailsford, P. Wynblatt, Acta Metall. (1979). https://doi.org/10.1016/0001-6160(79)90041-5
13. W. Lu, T.H. Andrew, A. Nor, B.R. Saffa, Build. Environ. (1996). https://doi.org/10.1016/0360-1323(96)00019-4
14. R. Pecora, J. Nanopart. Res. (2000). https://doi.org/10.1023/A:1010067107182
15. S.A. Slinn, W.G. Slinn, Atmos. Environ. (1982). https://doi.org/10.1016/0004-6981(82)90271-2
16. F. Chen, C.M. Simon, A.C.K. Lai, Atmos. Environ. (2006). https://doi.org/10.1016/j.atmosenv.2005.09.044
17. J.W. Tang, A.D. Nicolle, C.A. Klettner, J. Pantelic, L. Wang, A.B. Suhaimi, A.Y. Tan, G.W. Ong, R. Su, C. Sekhar, D.D. Cheong, PLOS one (2013). https://doi.org/10.1371/journal.pone.0059970
18. M.A. Shereen, S. Khan, A. Kazmi, N. Bashir, R. Siddique, J. Adv. Res. (2020). https://doi.org/10.1016/j.jare.2020.03.005
19. X. Li, Y. Shang, Y. Yan, L. Yang, J. Tu, Build. Environ. (2018). https://doi.org/10.1016/j.buildenv.2017.11.025

20. C. Cravero, D. Marsano, Indoor Built Environ. (2022). https://doi.org/10.1177/2F1420326X211039546
21. F. Mohamadi, A. Fazeli, Arch. Comput. Methods Eng. (2022). https://doi.org/10.1007/s11831-021-09706-3
22. M. Mirzaie, E. Lakzian, A. Khan, M.E. Warkiani, O. Mahian, G. Ahmadi, J. Hazard. Mater. (2021). https://doi.org/10.1016/j.jhazmat.2021.126587
23. M. Mesgarpour, J.M.N. Abad, R. Alizadeh, S. Wongwises, M.H. Doranehgard, S. Ghaderi, N. Karimi, J. Hazard. Mater. (2021). https://doi.org/10.1016/j.jhazmat.2021.125358
24. H. Wenjie, W. Kailu, H. Chi-Tim, C. Kai-Ming, T. Dominic, L. Raymond Wai-Man, H.X. Richard, Y. Eng-Kiong, H. Kin-Fai, C. Chun, J. Hazard. Mater. (2022). https://doi.org/10.1016/j.jhazmat.2022.129152
25. F. Salmani, M.R. Mahpeykar, E.A. Rad, Eur. Phys. J. Plus. (2019). https://doi.org/10.1140/epjp/i2019-12416-6
26. F. Salmani, E. Amiri Rad, M.R. Mahpeykar, J. Therm. Anal. Calorim. (2020). https://doi.org/10.1007/s10973-020-10526-z
27. E.C. Cole, C.E. Cook, Am. J. Infect. Control (1998). https://doi.org/10.1016/S0196-6553(98)70046-X
28. ANSI/ASHRAE Standard 55: Thermal environmental conditions for human occupancy
29. M.H. Dehghan, M. Abdolzadeh, Build. Environ. (2018). https://doi.org/10.1016/j.buildenv.2018.02.018